SLAC-PUB-7994, July 2000 T/E

Measurements of the Q^2-Dependence of the Proton and Neutron Spin Structure Functions g_1^p and g_1^n

The E155 Collaboration*: P. L. Anthony,[16] R. G. Arnold,[1,12] T. Averett,[5,◇] H. R. Band,[21] M. C. Berisso,[12] H. Borel,[7] P. E. Bosted,[1,12] S. L. Bültmann,[19] M. Buenerd,[16,†] T. Chupp,[13] S. Churchwell,[12,‡] G. R. Court,[10] D. Crabb,[19] D. Day,[19] P. Decowski,[15] P. DePietro,[1] R. Erbacher,[16,17] R. Erickson,[16] A. Feltham,[19] H. Fonvieille,[3] E. Frlez,[19] R. Gearhart,[16] V. Ghazikhanian,[6] J. Gomez,[18] K. A. Griffioen,[20] C. Harris,[19] M. A. Houlden,[10] E. W. Hughes,[5] C. E. Hyde-Wright,[14] G. Igo,[6] S. Incerti,[3] J. Jensen,[5] J. R. Johnson,[21] P. M. King,[20] Yu. G. Kolomensky,[5,12] S. E. Kuhn,[14] R. Lindgren,[19] R. M. Lombard-Nelsen,[7] J. Marroncle,[7] J. McCarthy,[19] P. McKee,[19] W. Meyer,[4] G. S. Mitchell,[21,×] J. Mitchell,[18] M. Olson,[9,□] S. Penttila,[11] G. A. Peterson,[12] G. G. Petratos,[9] R. Pitthan,[16] D. Pocanic,[19] R. Prepost,[21] C. Prescott,[16] L. M. Qin,[14] B. A. Raue,[8,18] D. Reyna,[1,○] L. S. Rochester,[16] S. Rock,[1,12] O. A. Rondon-Aramayo,[19] F. Sabatie,[7] I. Sick,[2] T. Smith,[13,×] L. Sorrell,[1] F. Staley,[7] S. St.Lorant,[16] L. M. Stuart,[16,§] Z. Szalata,[1] Y. Terrien,[7] A. Tobias,[19] L. Todor,[14] T. Toole,[1] S. Trentalange,[6] D. Walz,[16] R. C. Welsh,[13] F. R. Wesselmann,[14,19] T. R. Wright,[21] C. C. Young,[16] M. Zeier,[2] H. Zhu,[19] B. Zihlmann,[19]

[1] *American University, Washington, D.C. 20016*

[2] *Institut für Physik der Universität Basel, CH-4056 Basel, Switzerland*

[3] *University Blaise Pascal, LPC IN2P3/CNRS F-63170 Aubiere Cedex, France*

[4] *Ruhr-Universität Bochum, Universitätstr. 150, Bochum, Germany*

[5] *California Institute of Technology, Pasadena, California 91125*

[6] *University of California, Los Angeles, California 90095*

[7] *DAPNIA-Service de Physique Nucleaire, CEA-Saclay, F-91191 Gif sur Yvette, France*

---

*Work supported in part by Department of Energy contract DE–AC03–76SF00515

[8] *Florida International University, Miami, Florida 33199*

[9] *Kent State University, Kent, Ohio 44242*

[10] *University of Liverpool, Liverpool L69 3BX, United Kingdom*

[11] *Los Alamos National Laboratory, Los Alamos, New Mexico 87545*

[12] *University of Massachusetts, Amherst, Massachusetts 01003*

[13] *University of Michigan, Ann Arbor, Michigan 48109*

[14] *Old Dominion University, Norfolk, Virginia 23529*

[15] *Smith College, Northampton, Massachusetts 01063*

[16] *Stanford Linear Accelerator Center, Stanford, California 94309*

[17] *Stanford University, Stanford, California 94305*

[18] *Thomas Jefferson National Accelerator Facility, Newport News, Virginia 23606*

[19] *University of Virginia, Charlottesville, Virginia 22901*

[20] *The College of William and Mary , Williamsburg, Virginia 23187*

[21] *University of Wisconsin, Madison, Wisconsin 53706*

Abstract

The structure functions g_1^p and g_1^n have been measured over the range $0.014 < x < 0.9$ and $1 < Q^2 < 40$ GeV^2 using deep-inelastic scattering of 48 GeV longitudinally polarized electrons from polarized protons and deuterons. We find that the Q^2 dependence of g_1^p (g_1^n) at fixed x is very similar to that of the spin-averaged structure function F_1^p (F_1^n). From an NLO QCD fit to all available data we find $\Gamma_1^p - \Gamma_1^n = 0.176 \pm 0.003 \pm 0.007$ at $Q^2 = 5$ GeV^2, in agreement with the Bjorken sum rule prediction of 0.182 ± 0.005.

The spin-dependent structure function $g_1(x,Q^2)$ for deep-inelastic lepton-nucleon scattering is of fundamental importance in understanding the quark and gluon spin structure of the proton and neutron. The g_1 structure function depends both on x, the fractional momentum carried by the struck parton, and on Q^2, the squared four-momentum of the exchanged virtual photon. The fixed-Q^2 integrals (or first moments) $\Gamma_1^p(Q^2) = \int_0^1 g_1^p(x,Q^2)dx$ for the proton and $\Gamma_1^n(Q^2) = \int_0^1 g_1^n(x,Q^2)dx$ for the neutron are related to the net quark helicity $\Delta\Sigma$ in the nucleon. Measurements of Γ_1^p [1–4], Γ_1^d for the deuteron [2,3,5] (which essentially measures the average of the proton and neutron), and Γ_1^n [4,6–8] have found $\Delta\Sigma$ between 0.2 and 0.3, significantly less than the prediction [9] that $\Delta\Sigma = 0.58$ assuming zero net strange quark helicity and SU(3) flavor symmetry in the baryon octet. A fundamental sum rule originally derived from current algebra by Bjorken [10] predicts $\Gamma_1^p(Q^2) - \Gamma_1^n(Q^2) = g_A/6g_V$. Recent measurements are in agreement with this sum rule prediction when perturbative QCD (pQCD) corrections [11] are included.

According to the DGLAP equations [12], g_1 is expected to evolve logarithmically with Q^2, and in the case of g_1^p to increase with Q^2 at low x, and decrease with Q^2 at high x [3]. A similar Q^2-dependence has been observed in the spin-averaged structure functions $F_1(x,Q^2)$, while the ratio g_1/F_1 has been found to be approximately independent of Q^2 [3]. The precise behavior is sensitive to the underlying spin-dependent quark and gluon distribution functions. Fits to data for g_1 using NLO pQCD allow determinations of the first moments (from which the Bjorken sum rule can be tested) as well as the valence quark, sea quark, and gluon spin contributions. The goal of the present experiment (SLAC E155) was to make precise measurements over a wide range of Q^2 in a single experiment to further constrain these quantities.

The ratio of polarized to unpolarized structure functions can be determined from measured longitudinal asymmetries $A_\parallel$ using

$$g_1/F_1 = A_\parallel/d + (g_2/F_1)[(2Mx)/(2E-\nu)], \tag{1}$$

where $d = [(1-\epsilon)(2-y)]/\{y[1+\epsilon R(x,Q^2)]\}$, $y = \nu/E$, and $\nu = E-E'$, where E is the incident

and E' is the scattered electron energy in the lab frame, $\epsilon^{-1} = 1 + 2[1+\gamma^{-2}]\tan^2(\theta/2)$, $\gamma^2 = Q^2/\nu^2$, θ is the electron scattering angle, M is the nucleon mass, and $R(x,Q^2) = [F_2(x,Q^2)(1+\gamma^2)]/[2xF_1(x,Q^2)] - 1$ is typically 0.2 for the kinematics of this experiment [13]. For the contribution of the transverse spin structure function g_2 we used the twist-two result of Wandzura and Wilczeck (g_2^{WW}) [14]

$$g_2^{WW}(x,Q^2) = -g_1(x,Q^2) + \int_x^1 g_1(\xi,Q^2)d\xi/\xi, \tag{2}$$

evaluated using the empirical fit to g_1/F_1 given below (Eqs. 5 and 6). The g_2^{WW} model is in good agreement with existing data [3,15,16]. Using other reasonable models for g_2 that agree with existing data makes negligible changes to the extracted g_1/F_1 values due to suppression of the g_2 contribution by the factor $2Mx/(2E-\nu)$. The g_1 and g_2 structure functions are related to the virtual photon asymmetry $A_1 = (g_1/F_1) - \gamma^2(g_2/F_1)$ (which is bounded by $|A_1| \leq 1$).

In this Letter we report new measurements of g_1^p made using a 48.35 GeV polarized electron beam at SLAC. The new data extend to higher Q^2 (40 GeV^2) and lower x (0.014) than previous high statistics SLAC measurements [3]. Combined with measurements of g_1^d made in this same experiment using a ^{6}LiD target [5], we can extract g_1^n and compare with E154 [7] which measured g_1^n at similar kinematics using a polarized ^{3}He target as a source of polarized neutrons.

Longitudinally polarized electrons were produced by photoemission from a strained-lattice GaAs crystal. Beam pulses were typically 0.3 μs long, contained 2–4$\times 10^9$ electrons, and were delivered at a rate of 120 Hz. The helicity was selected randomly on a pulse-to-pulse basis to minimize instrumental asymmetries. The longitudinal beam polarization P_b was measured using Møller scattering from thin, magnetized ferromagnetic foils, periodically inserted about 25 m before the polarized target used to measure g_1. Results from two detectors (one detecting a single final-state electron, the other detecting two electrons in coincidence) agreed within errors, yielding $P_b = 0.813 \pm 0.020$.

As in E143 [3], the 3-cm-long polarized target cell contained pre-irradiated granules of

$^{15}NH_3$ immersed in liquid He at 1 K in a uniform magnetic field of 5 T. Microwaves near 140 GHz were used to drive the hyperfine transition which aligns (or anti-aligns) the nucleon spins with the magnetic field, producing proton polarizations of typically 90% in 10 to 20 minutes. The polarization slowly decreased due to radiation damage, and was periodically restored by annealing the target at about 80 K. The 2-3 mm diameter electron beam spot was rastered over the 3 cm^2 front surface of the target to uniformly distribute beam heating and radiation damage. To study possible experimental biases, the target polarization direction was periodically reversed using slight adjustments to the microwave frequency. Also, the direction of the magnetic field was reversed several times during the experiment. Final asymmetry results were consistent for the four polarization/field direction combinations.

The target polarization P_t was monitored with the same NMR Q-meter system as was used in experiment E143 [3]. The E143 design of target cell was modified for this experiment to improve the target polarization (average value of P_t was about 0.8 for E155) and this change had unforeseen effects on the performance of the NMR system when it was used to measure the proton polarization. Consequently, the NMR system was operated outside its design envelope, resulting in a significant degree of non-linear behavior. This problem is now qualitatively understood [17] but insufficient information about the NMR RF circuit parameters is available to allow adequate corrections for these non-linear effects to be calculated. Therefore the polarization data, for the proton target only, was extracted using the observed dependence of the polarization on the integrated beam dose deposited in the target material obtained primarily from experiment E155x [16]. This method leads to a larger systematic error in the proton polarization measurements (typically 7%) than would have been obtained using the standard NMR technique. It should be emphasized that this problem is unique to this particular set of proton experimental data and was eliminated in experiment E155x [16] by a further target cell design change.

Scattered electrons were detected in three independent magnetic spectrometers centered at angles of 2.75, 5.5, and 10.5 degrees. The two small angle spectrometers were the same as in E154 [7], while the large angle spectrometer was new for this experiment. It was

composed of a single dipole magnet and two quadrupoles, and covered $7 < E' < 20$ GeV, $9.6^\circ < \theta < 12.5^\circ$, and $-18 < \phi < 18$ mr, for a maximum solid angle of 1.5 msr at 8 GeV. Electrons were separated from a much larger flux of pions by using a gas Cherenkov counter and a segmented lead glass electromagnetic calorimeter.

The experimental asymmetries $A_\parallel$ were determined from

$$A_\parallel = \left(\frac{N_- - N_+}{N_- + N_+}\right) \frac{C_N}{f P_b P_t f_{RC}} + A_{RC}, \tag{3}$$

where the target polarization is parallel to the beam direction, N_- (N_+) is the number of scattered electrons per incident charge for negative (positive) beam helicity, $C_N \approx 0.985$ is a correction factor for the polarized nitrogen nuclei, f is the dilution factor representing the fraction of measured events originating from polarizeable hydrogen within the target, and f_{RC} and A_{RC} take into account radiative corrections.

The dilution factor f varied with x between 0.13 and 0.17; it was determined from a detailed model of the number of measured counts expected from each component of the target, including $^{15}NH_3$, various windows, NMR coils, liquid helium, etc. A typical target contained about 13% free protons, 66% ^{15}N, 10% ^{4}He, 6% Al, and 5% Cu-Ni by weight. The relative systematic error in f ranges from 2.2% to 2.6%.

A correction to the asymmetries was made for hadrons misidentified as electrons (typically 2% of electron candidates, but up to 15% in the lowest x bin of the 10.5° spectrometer). The correction used the asymmetry measured for a large sample of inclusive hadrons, which was found to be close to zero at all kinematics. An additional correction was made for electrons from pair-symmetric processes (such as e^+/e^- pair production from photons) measured by reversing the spectrometer polarity. The measured pair-symmetric $A_\parallel$ was consistent with zero at all kinematics, so the correction is equivalent to a dilution factor correction of typically 10% at the lowest E' of each spectrometer, decreasing rapidly to a negligible correction at higher E'.

Corrections were applied for the rate-dependence of the detector response, which changed the measured asymmetries by less than 1%. Corrections for kinematic resolution were gener-

ally a few percent or less, except for $x > 0.6$ where corrections to the measured asymmetries were as large as 15%.

The internal radiative corrections for $A_{\|}$ were evaluated using the formulae of Kuchto and Shumeiko [18]. The cross sections entering the asymmetry were 'externally radiated' according to Tsai [19]. Comparison of Born and fully radiated asymmetries allowed us to extract the asymmetry corrections f_{RC} and A_{RC}. By splitting the radiative correction into these two parts, we can propagate consistently the experimental error to the extracted Born asymmetries for the corresponding kinematic bins, in the presence of 'dilution' from elastic and inelastic radiative tails. Previous analyses (including E143) have used values of f_{RC} closer to unity by taking only quasi-elastic radiative tails into account, leading to smaller error bars at low x. Our new treatment is based on a definition of f_{RC} that insures that the additive correction A_{RC} is statistically independent from the data point to which it is applied. Values for f_{RC} range from 0.45 at the lowest x-bin to greater than 0.9 for $x > 0.15$, similar to the results in E154. However, the resulting net correction of the measured asymmetries is relatively small (0.01 to 0.02). The E155 radiative corrections are based on an iterative global fit to all available data, in which all previous SLAC data were re-corrected in a self-consistent way.

The E155 results for g_1^p/F_1^p and g_1^n/F_1^n are shown in Figs. 1 and 2 as a function of Q^2 at eleven values of x, and are listed in Table I. The neutron results were obtained from the proton results and E155 deuteron results [5] using

$$g_1^n = \frac{g_1^d}{1 - 1.5\omega_D} \frac{F_1^n + F_1^p}{F_1^d} - g_1^p \tag{4}$$

For the deuteron D-state probability we use $\omega_D = 0.05 \pm 0.01$, and F_1^p/F_1^n was obtained from the NMC fit [20]. Slight changes to the data of Refs. [1,2] were made to use the g_2^{WW} model [14] for g_2 instead of assuming $A_2 = 0$. Data from all experiments [1–4] have been matched to the x bins in Figs. 1 and 2 using the simple fit below for small bin centering corrections.

For the present experiment, most systematic errors (beam polarization, target polariza-

tion, fraction of polarizeable nucleons in the target) for a given target are common to all data and correspond to an overall normalization error of about 7.6% for the proton data. The remaining systematic errors (model dependence of radiative corrections, model uncertainties for $R(x,Q^2)$, resolution corrections) vary smoothly with x in a locally correlated fashion, ranging from a few percent for mid-range x bins, up to 15% for the highest and lowest bins.

Given the relatively large overall normalization uncertainty, the E155 data are in good agreement with the average of world data [1–4,6,7]. If we were to allow an overall normalization factor for our proton data, we would find a value of $1.08 \pm 0.03(\text{stat}) \pm 0.07(\text{syst})$.

In any given x bin, there is no evidence of strong Q^2 dependence for the ratio g_1/F_1. A simple parametric fit to world data with $Q^2 > 1$ GeV^2 (to mitigate possible higher twist contributions [21]) and missing mass $W > 2$ GeV (to avoid complications from the resonance region), shown as the dashed curves in all three figures, is given by

$$\frac{g_1^p}{F_1^p} = x^{0.700}(0.817 + 1.014x - 1.489x^2)(1 - \frac{0.04}{Q^2}) \tag{5}$$

$$\frac{g_1^n}{F_1^n} = x^{-0.335}(-0.013 - 0.330x + 0.761x^2)(1 + \frac{0.13}{Q^2}). \tag{6}$$

This fit has an acceptable χ^2 of 478 for 483 degrees of freedom. The coefficients of -0.04 ± 0.06 (0.13 ± 0.45) for the overall proton (neutron) Q^2 dependence are small and consistent with zero.

To examine the x dependence of g_1 at fixed Q^2, we averaged the E155 results over Q^2 assuming the Q^2 dependence of the fit above and use F_1 from [13,20] to obtain results for g_1^p and g_1^n at a fixed $Q^2 = 5$ GeV^2, shown in Fig. 3. The proton data suggest g_1 is approximately constant or slightly rising as $x \to 0$, but the neutron data are consistent with the trend of the E154 data to become increasingly negative at low x. The difference $g_1^p - g_1^n$ (which enters into the Bjorken sum rule) is theoretically expected to be well-behaved as $x \to 0$ compared to either g_1^p or g_1^n. This is because if isospin is a good symmetry, the sea quark and gluon contributions cancel, leaving only the difference of u and d quark valence distributions. The errors on the present data are too large to clearly support or contradict this expectation (see Fig. 3c).

The choice of low$-x$ extrapolation has a large impact on the the evaluation of the first moment of g_1. To be consistent with other analyses of g_1, we have made a NLO pQCD fit in the $\overline{MS}$ scheme to all recent data, using assumptions similar to those in [8]. The polarized parton distributions were parameterized as

$$\Delta f(x, Q_0^2) = A_f x^{\alpha_f} f(x, Q_0^2), \tag{7}$$

where $\Delta f = \Delta u_v$, Δd_v, $\Delta\overline{Q}$, and ΔG are the polarized valence, sea, and gluon distributions, and the $f(x, Q_0^2)$ are the unpolarized parton distributions at $Q_0^2 = 0.40$ GeV^2 from Ref. [22]. The positivity constraint $|\Delta f| < f$ was imposed in this fit, as well as the requirement $\alpha_f > 0$. The sea quark distributions were parameterized as $\Delta\overline{Q} = \frac{1}{2}(\Delta\overline{u} + \Delta\overline{d}) + \frac{1}{5}\Delta\overline{s}$. We assumed a symmetric quark sea for this analysis. We have not fixed the normalization of the non-singlet distributions, so that the fit results test the Bjorken sum rule. However, $\alpha_s(M_Z^2)$ has been fixed at 0.114 for consistency with the unpolarized distributions that were used [22]. The fit results are: $A_u = 0.95$, $A_d = -0.42$, $A_Q = 0.01$, $A_g = 0.50$, $\alpha_u = 0.57$, $\alpha_d = 0.0$, $\alpha_Q = 1.00$, and $\alpha_g = 0.02$. The overall χ^2/d.f. is 1.10 using statistical errors only. Evaluations of the fit are plotted as the solid curves in Figs. 1-3, and indicate only a slight dependence on Q^2 for g_1/F_1 in the x region where there are high statistics data. For $x < 0.014$, the proton and neutron fits become increasingly negative at fixed Q^2 (see Fig. 3), although the difference stays closer to zero and makes only a small contribution to the Bjorken sum rule.

Using the NLO pQCD fit, we find the quark singlet contribution $\Delta\Sigma = 0.23 \pm 0.04(\text{stat}) \pm 0.06(\text{syst})$ at $Q^2 = 5$ GeV^2, well below the Ellis-Jaffe prediction [9] of 0.58. We find $\Gamma_1^p = 0.118 \pm 0.004 \pm 0.007$, $\Gamma_1^n = -0.058 \pm 0.005 \pm 0.008$, and $\Gamma_1^p - \Gamma_1^n = 0.176 \pm 0.003 \pm 0.007$, in good agreement with the Bjorken sum rule prediction of 0.182 ± 0.005 evaluated with up to third order corrections in α_s [11]. For the first moment of the gluon distribution we obtain $\Delta G = 1.6 \pm 0.8 \pm 1.1$. The error on this quantity is too large to significantly constrain the gluon contribution to the nucleon spin sum rule.

In summary, the new data on g_1^p and g_1^n extend the range of high statistics electron

scattering results to lower x and higher Q^2 than previous data, improving the errors obtained from NLO pQCD fits to world data. The Bjorken sum rule prediction is validated within errors, while the extracted quark singlet contribution is small at approximately 0.2.

This work was supported by the Department of Energy (TJNAF, FIU, Massachusetts, ODU, SLAC, Stanford, Virginia, Wisconsin, and William and Mary); by the National Science Foundation (American, Kent, Michigan, and ODU); by the Schweizersche Nationalfonds (Basel); by the Kent State University Research Council (GGP); by the Commonwealth of Virginia (Virginia); by the Centre National de la Recherche Scientifique and the Commissariat a l'Energie Atomique (French groups).

REFERENCES

◇ Present address: College of William and Mary, Williamsburg, VA 23187

† Permanent Address: Institut des Sciences Nucléaires, IN2P3/CNRS, 38026 Grenoble Cedex, France

‡ Present Address: Duke University, TUNL, Durham, NC 27708

× Present Address: Los Alamos National Laboratory, Los Alamos, NM 87545

□ Present Address: Saint Norbert College, DePere, WI 54115

° Present Address: DESY, D-22603, Hamburg, Germany

§ Present Address: Lawrence Livermore National Laboratory, Livermore, CA 94551

[1] EMC, J. Ashman *et al.,* Nucl. Phys. B328 (1989), 1.

[2] SMC, D. Adeva *et al.,* Phys. Rev. D58 (1998) 112001.

[3] SLAC E143, K. Abe *et al.,* Phys. Rev. Lett. 74 (1995) 346; Phys. Rev. Lett. 75 (1995) 25; Phys. Lett. B364 (1995) 61; Phys. Rev. D58, 112003 (1998).

[4] HERMES, A. Airapetian *et al.,* Phys. Lett. B442 (1998) 484; Phys. Lett. B404 (1997) 383.

[5] SLAC E155, P. L. Anthony *et al.,* Phys. Lett. B463 (1999) 339.

[6] SLAC E142, P. L. Anthony *et al.,* Phys. Rev. D54 (1996) 6620.

[7] SLAC E154, K. Abe *et al.,* Phys. Rev. Lett. 79 (1997) 26.

[8] SLAC E154, K. Abe *et al.,* Phys. Lett. B405 (1997) 180.

[9] J. Ellis and R. Jaffe, Phys. Rev. D9 (1974) 1444; D10 (1974) 1669 (E).

[10] J. D. Bjorken, Phys. Rev. 148 (1966) 1467; Phys. Rev. D1 (1970) 1376.

[11] S. A. Larin and J. A. M. Vermaseren, Phys. Lett. B259 (1991) 345 and references therein.

[12] V. N. Gribov and L. N. Lipatov, Sov. J. Nucl. Phys. 15 (1972) 438, 675; Yu. L. Dokshitzer, Sov. Phys. JETP 46 (1977) 641; G. Altarelli and G. Parisi, Nucl. Phys. B126 (1977) 298.

[13] K. Abe *et al.,* Phys. Lett. B452 (1999) 194.

[14] S. Wandzura and F. Wilczek, Phys. Lett. B72 (1977) 195.

[15] SLAC E155, P. L. Anthony *et al.,* Phys. Lett. B458 (1999) 529.

[16] SLAC E155x, to be published.

[17] G. R. Court and M. Houlden, in proceedings "Workshop on NMR in Polarized Targets", S. Bültmann and D. G. Crabb, ed., Charlottesville, VA 1998.

[18] T. V. Kuchto and N. M. Shumeiko, Nucl. Phys. B219 (1983) 412; I. V. Akusevich and N. M. Shumeiko, J. Phys. G20 (1994) 513.

[19] Y. S. Tsai, Report No. SLAC–PUB–848, 1971; Y. S. Tsai, Rev. Mod. Phys. 46 (1974) 815.

[20] NMC, M. Arneodo *et al.,* Phys. Lett. B364 (1995) 107.

[21] I. I. Balitsky, V. M. Braun and A. V. Kolesnichenko, Phys. Lett. B242 (1990) 245; B318 (1993) 648 (E); X. Ji and P. Unrau, Phys. Lett. B333 (1994) 228; E. Stein, P. Gornicki, L. Mankiewicz, A. Schafer, Phys. Lett. B353 (1995) 107.

[22] M. Gluck, E. Reya, A. Vogt, Eur. Phys. J. C5 (1998) 461.

FIGURES

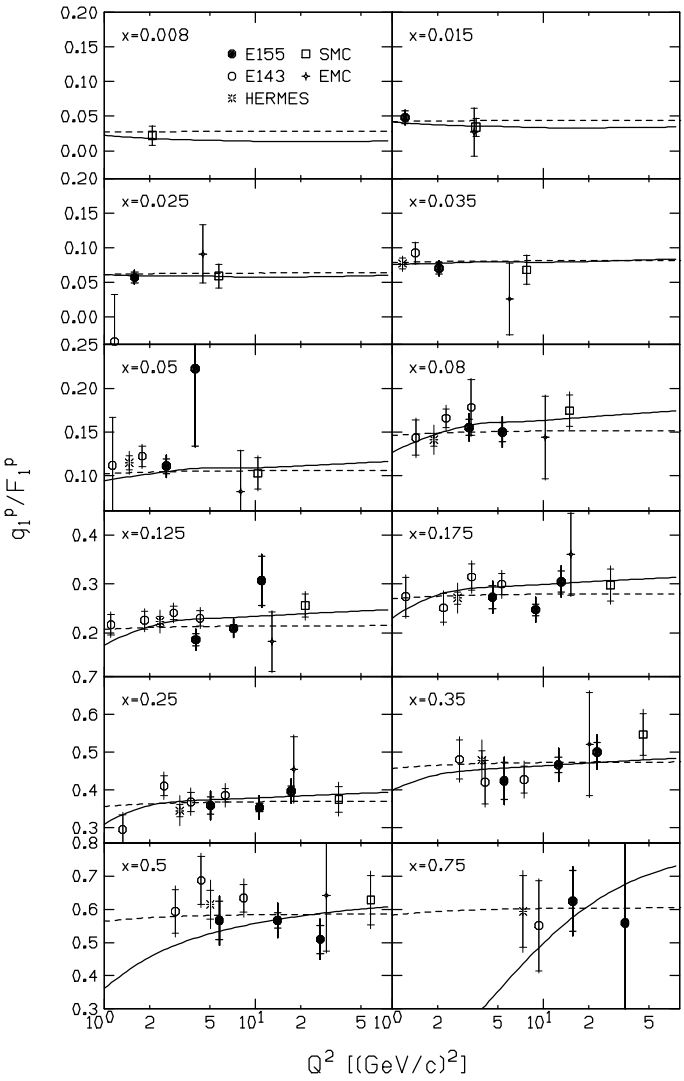

FIG. 1. Ratios g_1^p/F_1^p extracted from experiments assuming the g_2^{WW} model for g_2. Inner errors are statistical only, while systematic errors are included in quadrature in the outer error bars. The solid curves correspond to the NLO QCD fit described in the text, while the dashed curves are from the simple fit given by Eq. 5.

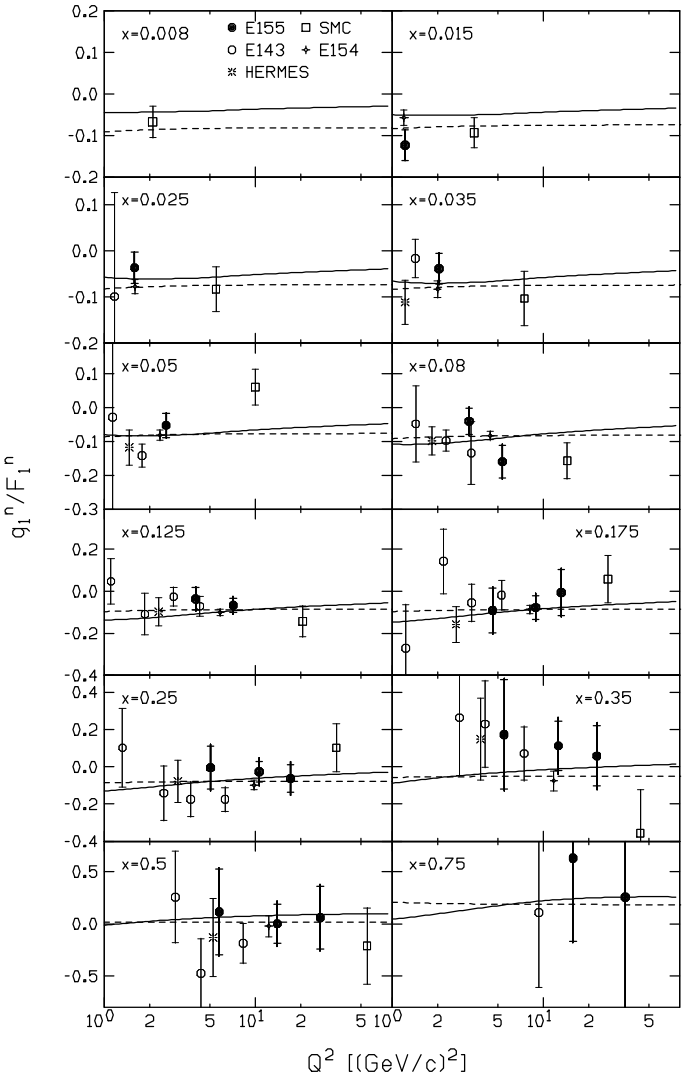

FIG. 2. Same as Fig. 1 except for g_1^n/F_1^n and Eq. 6 for the dashed curves.

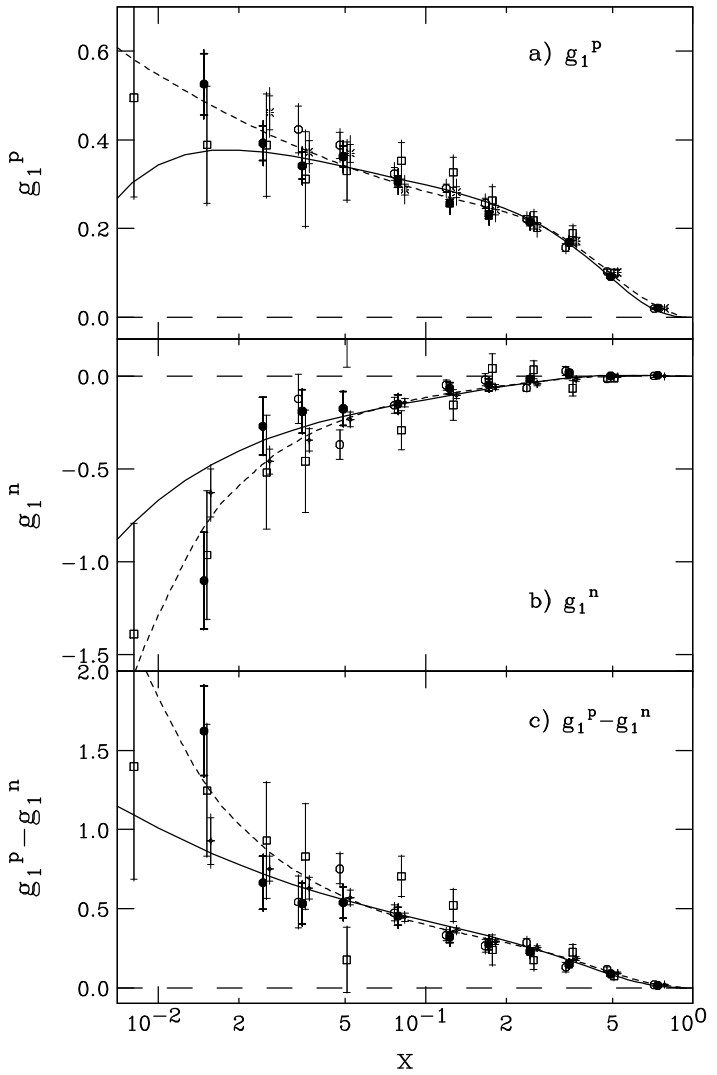

FIG. 3. Data for g_1^p (a), g_1^n (b), and $g_1^p - g_1^n$ (c), evaluated at $Q^2 = 5$ GeV^2. The data are from this experiment (solid circles), E143 (open circles), SMC (squares), HERMES (stars), and E154 (crosses). The $g_1^p - g_1^n$ values were obtained from the proton and deuteron results of E155, E143, and SMC, while the proton E155 and neutron E154 results were used to obtain the results with the cross symbol. The curves are as in Figs. 1 and 2.

TABLES

TABLE I. Results for g_1/F_1 from this experiment for the proton and neutron for $E = 48.35$ and the indicated values of x and Q^2.

$< x >$	Q^2	g_1^p/F_1^p	g_1^n/F_1^n
	(GeV^2)	$\pm$ stat. $\pm$ syst.	$\pm$ stat. $\pm$ syst.
0.015	1.22	0.048 $\pm$ 0.009 $\pm$ 0.004	-0.125 $\pm$ 0.037 $\pm$ 0.006
0.025	1.59	0.057 $\pm$ 0.008 $\pm$ 0.006	-0.038 $\pm$ 0.034 $\pm$ 0.007
0.035	2.05	0.070 $\pm$ 0.008 $\pm$ 0.007	-0.040 $\pm$ 0.034 $\pm$ 0.008
0.050	2.58	0.111 $\pm$ 0.009 $\pm$ 0.009	-0.054 $\pm$ 0.036 $\pm$ 0.011
0.050	4.01	0.222 $\pm$ 0.088 $\pm$ 0.009	-0.852 $\pm$ 0.400 $\pm$ 0.012
0.080	3.24	0.155 $\pm$ 0.009 $\pm$ 0.013	-0.039 $\pm$ 0.038 $\pm$ 0.016
0.080	5.36	0.150 $\pm$ 0.011 $\pm$ 0.013	-0.157 $\pm$ 0.048 $\pm$ 0.017
0.125	4.03	0.186 $\pm$ 0.012 $\pm$ 0.018	-0.034 $\pm$ 0.052 $\pm$ 0.024
0.125	7.17	0.209 $\pm$ 0.007 $\pm$ 0.018	-0.066 $\pm$ 0.034 $\pm$ 0.025
0.125	10.99	0.307 $\pm$ 0.051 $\pm$ 0.018	-0.425 $\pm$ 0.238 $\pm$ 0.028
0.175	4.62	0.273 $\pm$ 0.023 $\pm$ 0.023	-0.088 $\pm$ 0.106 $\pm$ 0.035
0.175	8.90	0.247 $\pm$ 0.012 $\pm$ 0.023	-0.077 $\pm$ 0.056 $\pm$ 0.036
0.175	13.19	0.305 $\pm$ 0.022 $\pm$ 0.023	-0.010 $\pm$ 0.109 $\pm$ 0.039
0.250	5.06	0.358 $\pm$ 0.023 $\pm$ 0.030	-0.007 $\pm$ 0.114 $\pm$ 0.053
0.250	10.64	0.353 $\pm$ 0.011 $\pm$ 0.030	-0.027 $\pm$ 0.056 $\pm$ 0.055
0.250	17.21	0.396 $\pm$ 0.014 $\pm$ 0.030	-0.069 $\pm$ 0.075 $\pm$ 0.057
0.350	5.51	0.424 $\pm$ 0.049 $\pm$ 0.039	0.164 $\pm$ 0.288 $\pm$ 0.079
0.350	12.60	0.466 $\pm$ 0.020 $\pm$ 0.039	0.103 $\pm$ 0.130 $\pm$ 0.082
0.350	22.73	0.500 $\pm$ 0.025 $\pm$ 0.038	0.055 $\pm$ 0.161 $\pm$ 0.086
0.500	5.77	0.561 $\pm$ 0.058 $\pm$ 0.048	0.155 $\pm$ 0.417 $\pm$ 0.117
0.500	14.02	0.561 $\pm$ 0.024 $\pm$ 0.048	0.017 $\pm$ 0.187 $\pm$ 0.123
0.500	26.86	0.507 $\pm$ 0.042 $\pm$ 0.048	0.057 $\pm$ 0.309 $\pm$ 0.125

0.750	15.70	$0.622 \pm 0.091 \pm 0.050$	$0.616 \pm 0.775 \pm 0.144$
0.750	34.72	$0.559 \pm 0.405 \pm 0.050$	$0.254 \pm 3.141 \pm 0.138$